optica

Portable simultaneous vision device to simulate multifocal corrections

CARLOS DORRONSORO,* AISWARYAH RADHAKRISHNAN, JOSE RAMON ALONSO-SANZ, DANIEL PASCUAL, MIRIAM VELASCO-OCANA, PABLO PEREZ-MERINO, AND SUSANA MARCOS

Laboratory of Visual Optics and Biophotonics, Instituto de Optica, CSIC, 28006 Madrid, Spain
**Corresponding author: cdorronsoro@io.cfmac.csic.es*

Received 18 February 2016; revised 16 June 2016; accepted 29 June 2016 (Doc. ID 259377); published 18 August 2016

Multifocal lenses are increasingly used solutions for presbyopia, the age-related loss of crystalline lens focus ability. These lenses work by the principle of simultaneous vision, superimposing focused and defocused images on the retina. Providing the experience of simultaneous vision to a patient before permanent implantation of a multifocal lens is a recognized unmet need to increase the patient's confidence and optimize the lens selection. We developed a hand-held, see-through multifocal vision simulator based on temporal multiplexing of a tunable lens. The device was calibrated and validated using focimetry and Hartmann–Shack aberrometry revealing high reproducibility of the through-focus multifocal energy distribution and high optical quality. We measured visual acuity and perceptual quality on nine cyclopeged patients with three monofocal, two bifocal, and two trifocal corrections with different far/intermediate/near energy distributions simulated using the device. Visual performance and perceptual quality with multifocal corrections varied across patients, although they were more uniform across distances than monofocal corrections. Among the bifocal and trifocal designs, a trifocal with more energy at far was the most frequently identified as providing better quality. The simultaneous vision simulator proved a promising compact tool to study visual performance with multifocal corrections and to select the lens design best suited for each patient, alternative to costly and bulky adaptive optics based devices.

OCIS codes: (330.0330) Vision, color, and visual optics; (330.4300) Vision system - noninvasive assessment; (330.4460) Ophthalmic optics and devices; (330.4595) Optical effects on vision; (330.7327) Visual optics, ophthalmic instrumentation.

http://dx.doi.org/10.1364/OPTICA.3.000918

1. INTRODUCTION

There is an increasing proportion of presbyopes in the population demanding treatments that provide comfortable vision at all distances. An increasingly used solution for presbyopia is multifocal designs, using diffractive or refractive profiles, resulting in bifocal, trifocal, and extended-depth-of-focus designs. These corrections, generally delivered in the form of contact lenses, intraocular lenses, or corneal laser ablation patterns, produce a retinal image that has superimposed blurred and sharp images at all distances. Most clinical studies are limited to reports of visual acuity or contrast sensitivity in patients with multifocal corrections measured at different distances, or patient satisfaction questionnaires, generally aiming at finding to what extent near vision is improved without compromising distance vision, when compared to a monofocal lens [1–5].

Visual simulators of multifocal corrections allow undertaking systematic studies of visual performance with multiple lens designs, which can be directly compared by the patient. These simulators work by projecting the equivalent phase maps of a multifocal lens noninvasively directly onto the patient's pupil plane. Most visual simulators are based on adaptive optics elements, for example, deformable mirrors or spatial light modulators [6–9]. The systems can operate in a closed loop (i.e., a wavefront sensor continuously monitors the aimed combined wave aberration of the eye and correction, and the actuators of a deformable mirror respond to maintain this correction) or statically (i.e., a given correction is programmed in a pixelated reflective phase-only spatial light modulator) [6]. Visual stimuli are generally projected in a display in the system, allowing the subject to perform psychophysical tasks under the programmed corrections [10–12].

We have recently presented two-channel visual simulators, which allow visual simulation of bifocal corrections. In these systems, two channels, one focused at far and the other one focused at near, are combined at the pupil plane, simulating a pure simultaneous vision correction [13], or in combination with a transmission spatial light modulator and polarizers, simulating refractive corrections of different pupillary pattern distributions for near and far. A study systematically investigating the effect of the magnitude of the near addition on visual acuity revealed that intermediate additions (around 2 D) deteriorated far vision more than lower or higher additions [13]. Corrections with different distributions of near and far regions across the pupil resulted in different visual performance in the same patient, indicating that not all corrections (even with the same addition and energy ratio for far and near) are perceptually similar [14]. Furthermore, the best perceived quality with an angularly segmented bifocal design is biased by the actual orientation in which the lens is placed, likely affected by the actual combination of the correction and the patient's optics [15]. Using visual simulators, we also found that subjects can adapt to bifocal corrections [16].

Current visual simulators [6–9] allow rapid simulation of multiple multifocal corrections, allowing the same patient to compare across designs. But the use of current devices is mostly limited to experimental environments, given their relatively high dimensions, and that they do not allow experiencing the real world through the simulated multifocal correction, but rather small (typically <2 deg) visual field projections. Visual simulators have proved efficient tools for understanding multifocal vision and to help in the design of new multifocal profiles. However, they hold great promise as a clinical tool in daily cataract surgery or contact lens practice where clinicians and patients face the decision of opting for a multifocal correction. These systems offer the possibility of testing a lens design before it is implanted, or narrowing down the contact lens of choice in a generally lengthy trial-and-error procedure.

In this study, we report the development and use of a new hand-held see-through simultaneous vision simulator, based on a novel temporal-multiplexing approach using electronically tunable lenses, which allowed the simulation of different multifocal lens profiles. The device was tested on subjects who performed visual acuity, perceptual scoring, and perceptual performance under simulated monofocal, bifocal, and trifocal simultaneous vision corrections.

2. METHODS

A. Portable Simultaneous Vision Simulator

A hand-held simultaneous vision simulator was developed, whose active component is an optomechanically tunable lens (EL-10-30, Optotune Inc., Switzerland), working in temporal multiplexing [17,18]. Figure 1A shows a schematic view of the system. The tunable lens (TL) is conjugated with the subjects' pupil using a pair of achromatic doublets (75 mm EFL) acting as relay lenses. The distance between doublets can be adjusted to correct the spherical refraction of the patient. Two pairs of mirrors (M3–M6, Fig. 1A) emulate two Porro prisms to project upright images on the subjects' retina. M1, M2 are used to place the image, covering 14 deg of visual field, in the line of sight of the viewer, so the patient has a natural view of the external world through the system. Figure 1B shows a photo of the working prototype. Figure 1C shows the system with its cover, and being used by a patient. The tunable lens is controlled by a custom-developed electronic driver, based on Arduino Nano 3.0 (Arduino, Italy), whose firmware is programmed using C. The driver provides the tunable lens with a PWM signal at 60 KHz with tunable duty cycle, to change the current between 0 and 150 mA, inducing optical power shifts between −1.50 D and +6 D (using a negative offset lens). The temporal pattern of the variation defined the through-focus energy profile of the lens. Multifocality is simulated by rapidly varying the optical states of the lens, controlling the state of the lens (focus position) and the amount of time the lens remains in any given state (energy dedicated to a particular focus). This variation is faster than the visual fusion frequency, so the temporal multiplexing produces retinal images that are perceptually static. For example, for a 70% far and 30% near bifocal lens two optical states are induced in a 20 ms time period, with the far state induced for 14 ms and the near state for 6 ms, in a pattern repeated over time. The instrument provides pure simultaneous vision, in which the entire pupil provides far, intermediate, and near vision, as in diffractive designs. This system does not replicate the pupillary power distributions found in refractive segmented designs, although it can simulate the corresponding through-focus energy profile.

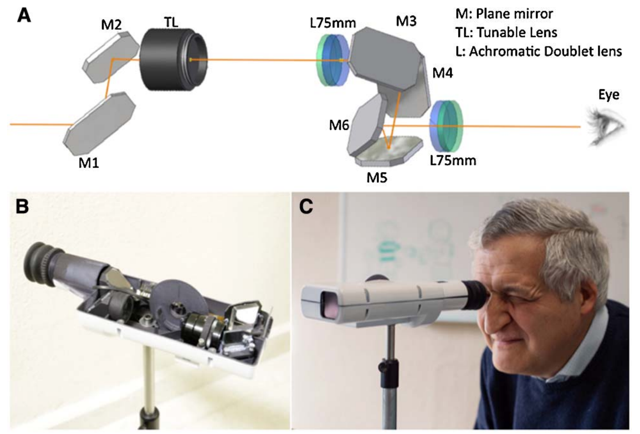

Fig. 1. A: Schematic of miniaturized simultaneous vision simulator. The image formed by the tunable lens (TL) is projected onto the eye using a pair of achromatic doublets of 75 mm EFL. M1, M2 are used to align the optical axis of the device with the line of sight of the eye. Mirrors M3–M6 act as a pair of Porro prisms for image re-erection. B: SimVis Mini prototype showing principal components. C: Subject viewing through SimVis Mini.

B. Tunable Lens Calibrations

The voltage-diopter reciprocity of the tunable lens was characterized by imaging a standard ETDRS visual acuity chart (Early Treatment Diabetic Retinopathy Study chart) placed at distance of 3 m, through the tunable lens and a Badal system, by a CCD camera with a high numerical aperture objective focused at infinity. Defocus introduced by the Badal system (each 0.25 D) was compensated by changing the voltage of the tunable lens.

The optical aberrations induced by the tunable lens in different focus positions were also measured using a Hartmann–Shack wavefront sensor incorporated in a custom-developed adaptive optics system [19,20]. The tunable lens was placed (vertically) at a conjugate pupil plane of the system, and the change in the lower- and higher-order Zernike coefficients was documented.

The ability of the tunable lens to represent bifocal and trifocal optical designs was tested using a custom-developed high-speed focimeter, based on laser ray tracing [21]. A ring-shaped beam of eight rays generated by a two-mirror galvanometer deflecting a laser beam (each ray traced for 1.25 ms) was imaged through monofocal, bifocal, and trifocal states of the tunable lens, using a CMOS camera with adjustable exposure time (down to 1 ms).

All optical calibrations were performed with a fixed pupil diameter of 6 mm, obtained with a diaphragm placed next to the tunable lens.

C. Simulated Lenses

Three monofocal, two bifocal, and two trifocal corrections were simulated using the simultaneous vision simulator. The monofocal corrections were 100%Far (100F), 100%Intermediate (100I), and 100%Near (100N); the bifocal corrections were 50%Far and 50%Near (50F/50N) and 70%Far and 30%Near (70F/30N); and the trifocal corrections assessed were 33%Far/33% Intermediate/33%Near (33F/33I/33N) and 50%Far/20% Intermediate/30%Near (50F/20I/30N). For all subjects, the far distance focus was set to their best subjective focus (which corrected their spherical refractive error) determined by a bracketing technique. The intermediate focus was set to 1.5 D, and the near focus was set to 3 D.

D. Visual Scenes

A real visual scene was simulated in a laboratory environment, with targets at far (4 m), intermediate (66 cm), and near (33 cm). For visual acuity measurements, a visual acuity chart displayed using an iPAD [Fig. 2A] with retina display (maximum luminance 119 cd/m^2, 264 ppi, 9.7″) was placed at the different distances. For perceptual measurements, the visual scene consisted of a poster of a landscape (subtending 4 deg at the retina) and a high-contrast letter (logMAR 1) at far, covering the upper right quarter of the visual field, a laptop with high-contrast text (4 deg angular subtense) at intermediate distance (maximum luminance 117 cd/m^2, 116 ppi, 13.3″) covering the upper left quadrant, and a mobile phone with the same high-contrast text (maximum luminance 128 cd/m^2, 342 ppi, 4.3″) covering the inferior zone (6 deg angular subtense) at near distances. For near and intermediate distance the same continuous text of nonserif letters was used; the size of the letters at near was 14 pt, and at intermediate distance it was 18 pt. In total, 30% of the visual scene was dedicated for far vision, 30% for intermediate vision (4 deg), and 40% for near vision [Fig. 2B]. As all distances are presented at the same time, the subject can provide an average response of the perceptual quality at all distances at once.

E. Subjects

Measurements were performed on nine subjects, with an age range of 20–62 years. In all subjects (except one presbyope), presbyopia was pharmacologically simulated by instilling one drop of 1% tropicamide three times, 15 min prior to measurements and hourly. The artificial pupil of the instrument was set to 5 mm diameter. The experimental session lasted 2 h. Mean spherical refractive error ranged from −5.50 D to +2.75 D. None of the subjects had astigmatism >1 D. The experiments conformed to the tenets of the Declaration of Helsinki, with protocols approved by the Consejo Superior de Investigaciones Científicas Ethics Committee. All participants provided written informed consent.

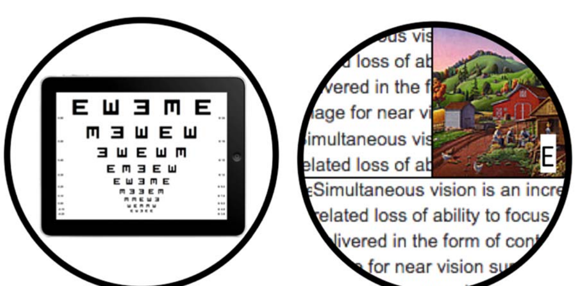

Fig. 2. A: Visual acuity measurements using commercial software application displayed in a HD display. B: Perceptual preference measurements using visual scene with landscape for far and a high-contrast text for intermediate and near distances.

F. Visual Acuity Measurements

LogMAR visual acuity was evaluated at all distances under the simulated corrections using a commercial software application (Fast acuity XL, Kybervision Inc.) controlled using and displayed in the portable HD display device described above. Tumbling *E* letters at four orientations were displayed [Fig. 2A], and the visual acuity was measured as the smallest size of letters that could be resolved by the subjects. Visual acuity was assessed at the three distances in random order and averaged across subjects according to [22].

G. Perceptual Score Measurements

The perceived image quality of the global visual scene (overall score) and at far, intermediate, and near distances was judged by the subject using a perceptual scoring technique [16]. The subject viewed the visual scene [Fig. 2B] through each optical correction presented in random order. For each presentation, the subject scored the visual scene from very blurred (score 0) to very sharp (score 5). The measurements were repeated three times, and the average score was calculated for each refractive option (simulated lens and observation distance) induced.

H. Preference Measurements

The preference to a specific multifocal vision correction was tested using a two alternative forced choice procedure [23,24] in pairwise comparisons between corrections. Subjects viewed the visual scene for 5 s through a correction and subsequently viewed the same scene through another correction for 5 s. The six combinations of the two bifocal and two trifocal corrections (50F/50N, 70F/30N, 33F/33I/33N, and 50F/20I/30N) were tested in random order. The chosen correction of the pair was given a score of +1, and the other correction in the pair was given a score of −1. The measurements were repeated 10 times, and the sum score was calculated for each correction. For testing the significance of the preference of a given correction, Bernoulli cumulative distribution function statistics was used as a null hypothesis (corresponding to random choices), with a significance level of 0.05 [25]. Any score greater than +10 (out of +30 possible) indicates significant preference, and −10 indicates (out of −30) significant rejection.

3. RESULTS

A. Optical Characterization of the Simultaneous Vision Device

As shown in Fig. 3A, the voltage and defocus induced show an almost linear relationship (within the 0.25 diopter step used in the induction). A voltage increment around 0.5 V is needed to compensate with the tunable lens each diopter of defocus induced in the Badal channel.

As expected, aberrations of the tunable lens increased with an increase in the power, as shown in Fig. 3B. Solid symbols stand for horizontal aberrations, while empty symbols stand for vertical

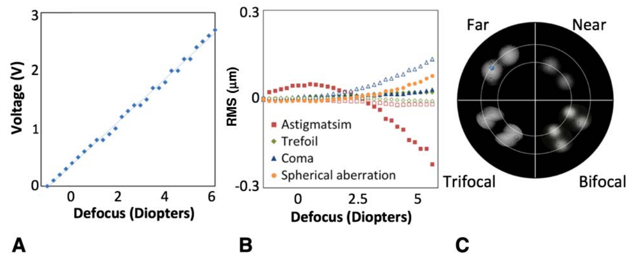

Fig. 3. A: Voltage versus induced defocus. B: Measured lower- and higher-order aberrations (RMS in micrometers) with induced defocus. Solid symbols stand for horizontal aberrations, while empty symbols stand for vertical aberrations. C: Laser spots at the CMOS camera of the high-speed focimeter, corresponding to monofocal and multifocal corrections. Outer circle stand for far vision optical power. Inner circle stands for near vision optical power. See text for details.

aberrations. As the lens is in the vertical position, the vertical aberrations account for the asymmetric effect of gravity on the membrane and therefore on the wavefront. The change in root mean square of astigmatism and other higher-order terms were clinically irrelevant within a range of 5 D induced (<0.05 µm for 6 mm pupils, equivalent to the repeatability of wavefront measurements on real eyes). As mentioned, the subsequent measurements on real eyes were performed with 5 mm pupils and 3 D additions.

Figure 3C shows laser spots at the CMOS camera of the high-speed focimeter, corresponding to the rays traced through the tunable lens. The simulated monofocal corrections for far vision (top-left quadrant) and for near vision (top-right quadrant) direct the rays to different positions (outer and inner dotted circles, respectively). The power of the lens is proportional to the ring diameter. Bifocal (bottom-right) and trifocal (bottom-left) corrections produce the same diameters (dotted circles), indicating a similar optical power and addition induced in static and dynamic regimes. Moreover, when the bifocal correction is observed at long exposure times, two clearly separated spots are seen (with no light in between them) indicating that the transition between one foci and the other is quick enough, and no energy loss is captured by the camera. At very short exposure times (and high power in the laser) the camera captures either one spot (corresponding to one foci) or the other, with a transition time limited to less than 1 ms.

A visual inspection through the portable simultaneous vision simulator confirmed that the temporal multiplexing was fast enough to produce temporal fusion, and that all the simulated lenses produced images of the visual scene with a static appearance in the retina, without flicker or oscillations.

B. Visual Acuity with Simulated Multifocal Corrections

Figure 4A shows the logMAR visual acuity at far versus at near, averaged [22] across subjects ($N = 9$). The size of the bubbles represents the intermediate visual acuity. Each color represents a different simulated correction. There is a linear change in visual acuity for far and near across the designs. As the percentage of energy at far increased for a given design (the extreme being a monofocal design focused at far, 100F), visual acuity increased at far ($r = -0.96$, $p < 0.0001$) and decreased at near ($r = 0.76$, $p < 0.0001$) linearly. Figure 4B represents the range of visual acuity for far to near, for each design, with the green square representing visual acuity at intermediate distance. Monofocal

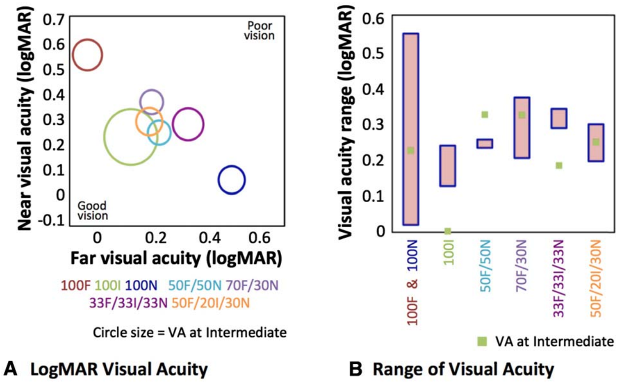

Fig. 4. A: logMAR visual acuity at far versus at near with different monofocal and multifocal corrections, averaged across nine subjects. Each color represents a different correction. The size of the bubble represents VA at intermediate distance. B: Range of visual acuity for far and near with different monofocal and multifocal corrections, averaged across nine subjects. Green squares represent visual acuity at intermediate distance.

corrections (100F and 100N) provide good visual acuity when in focus (mean logMAR 0.015 ± 0.03) with compromised visual acuity at the nonfocused distance (mean logMAR VA 0.51 ± 0.23). On the other hand, the monofocal intermediate correction (100I) and the simultaneous vision corrections provided moderate visual acuity at all distances. Among these corrections, the multifocal benefit calculated as the average of visual acuity at the three distances was highest for 100I (logMAR VA 0.12 ± 0.04). The multifocal corrections 50F/50N, 70F/30N, 33F/33I/33N, and 50F/20I/30N had an average multifocal benefit of logMAR 0.27 ± 0.05, 0.3 ± 0.09, 0.27 ± 0.08, and 0.25 ± 0.05, respectively.

C. Perceptual Score of Multifocal Corrections

The average perceptual score varied systematically across designs [Fig. 5A]. The perceived quality at far or near correlated significantly and strongly with the percentage of energy devoted to far or near in each correction ($r = 0.92$, $p < 0.0001$). The overall perceptual score correlated significantly with the intermediate ($r = 0.65$, $p < 0.0001$) and far ($r = 0.51$, $p < 0.001$) perceptual scores, but not with the near perceptual score ($r = -0.07$, $p = 0.57$). On average, the overall perceptual score was maximum for the 100I correction (score 3.5 ± 0.6) among the monofocal corrections and was maximum for 50F/20I/30N (score

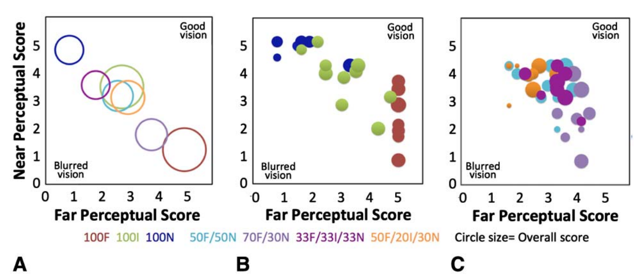

Fig. 5. Perceptual score at far and near distances. Bubble size indicates overall score. A: Average across subjects for all corrections. B: For monofocal corrections in all subjects. C: For simultaneous vision corrections in all subjects.

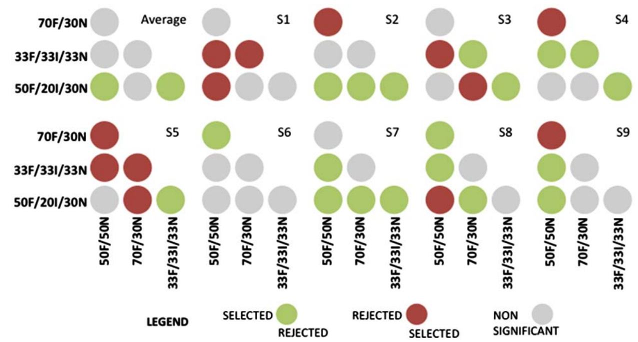

Fig. 6. Preference maps for simultaneous vision corrections. Green dot indicates that the design indicated in the left label (horizontally oriented text) was preferred significantly over the one in the lower label (vertically oriented text), and a red dot indicates that the design indicated in the left label was significantly rejected compared to the one in the lower label. Gray dots indicate nonsignificant preferences.

2.7 ± 0.6) among the multifocal corrections. The mean score across subjects at intermediate distance ranged from 4.8 (100I) to 1.7 (50F/50N)—2.2 on average across corrections (excluding 100I). Figure 5B shows the perceptual scores for individual subjects for the monofocal corrections (red, green, and blue bubbles represent far, intermediate, and near corrections). For 100F, the perceptual score was 5 in all subjects at far, but for the same correction at near it ranged from 0 to 3. Similarly, the perceptual score for 100 N ranged from 4 to 5 at near, and at far it ranged from 0 to 3. Monofocal intermediate correction showed the largest range of perceptual scores across subjects at far (1.7–3.3) and near (1.3–5) distances, indicating large intersubject variability in the responses. On the other hand, the multifocal corrections [Fig. 5C] had a similar range of perceptual scores at far and near distances. Specifically, the 33F/33I/33N showed the narrowest range at far (2–4), and 50F/20I/30N had the smallest range at near (2.1–4.3).

D. Preference Results

Preference maps (Fig. 6) were generated to identify significant preferences in each pairwise comparison, for simultaneous vision corrections. Assuming Bernoulli's distribution, green dots indicate that the design indicated in the right label (horizontally oriented text) was preferred significantly over the one in the lower label (vertically oriented text), and a red dot indicates that the design indicated in the right label was significantly rejected compared to the one in the lower label. Gray dots indicate nonsignificant preferences. When the pooled responses from all subjects are considered simultaneously (marked as "Average" preference map in Fig. 6), 50F/20I/30N was preferred significantly over other designs. However, as shown in Fig. 6, preference maps from individual subjects clearly show high intersubject variability and are different from the average trend.

4. DISCUSSION

The frequency of choosing a multifocal correction as a treatment of presbyopia, as well as the number of designs commercially available, is rapidly increasing. However, how the world looks through a multifocal correction is not easy to imagine. Clinicians often fail at offering a multifocal solution to a patient if they subjectively believe that the patient may not be satisfied post-operatively, or if they find unsatisfied patients following multifocal IOL implantations. Contact lens specialists often rely on a trial-and-error approach, trying multiple contact lens designs until the optimal solution is identified. We have presented a novel portable through-focus simultaneous vision simulator that allows experiencing the real world through realistic optical simulations of multifocal corrections. The system holds promise as a tool to help in selecting the optimal treatment for the patient.

Visual and perceived visual quality with monofocal corrections. In our study, we evaluated visual acuity and perceived visual quality with monofocal designs at far, intermediate, and near distances. Both metrics varied similarly across conditions. As expected, the monofocal corrections at far and at near provided the maximum quality for the corresponding distance in focus and drastically reduced the visual acuity at the other distance. The monofocal intermediate correction decreased far and near visual acuity, though to a lesser extent, and provided an acceptable intermediate vision. This result agrees with reports in eyes implanted with monofocal and multifocal IOLs [2,3,5]. In fact, monofocal lenses outperformed multifocal designs at both far and intermediate, although not at near. However, the higher intersubject variability performance with monofocal designs focused at intermediate distance suggests that, while this may be a possible approach to treat presbyopia in some subjects, this is not by any means optimal for all subjects.

Visual acuity and perceived visual quality with multifocal corrections. We evaluated visual acuity and perceived visual quality with two bifocal and two trifocal designs, which had an equal energy distribution across distances or had larger energy dedicated for far. The multifocal visual benefit was, on average, 1.1 times higher with the multifocal corrections than with the monofocal corrections at far or near. Trifocal corrections provided, as expected, higher visual acuity at the intermediate distance compared to bifocal corrections. On average, the bifocal correction with equal energy between far and near and the far dominant trifocal correction provided better overall performance than the other lenses. Thus both visual acuity and perceptual score vary across subjects as expected from the optical principles of each design. However, the overall perceptual scores for both monofocal and multifocal corrections varied over a wide range (from 4.8 to 1) across subjects. These perceptual differences in responses found across subjects [Figs. 5B and 5C] are likely due to intersubject differences in the optics, neural processing, or differences in visual needs.

Pattern preferences to simultaneous vision corrections. Direct comparisons of each multifocal design against others revealed general trends, as well as statistically significant differences across subjects. As a general trend, the trifocal design that was far dominant (50F/20I/30N) was preferred over other simultaneous designs. On the other hand, a trifocal design that provided very low energy at far (33F/33I/33N) compared to the other designs was systematically rejected by the subjects. A bifocal 50F/50N design produced in general better visual response than other configurations, although specific preferences/rejections were highly subject-dependent. While the visual scene was constructed to represent a realistic environment at different distances, it is true that the frequency content and the distribution of targets at each distance may have somewhat influenced the results, and responses may have differed with a different visual scene.

Those changes may reflect different visual needs across subjects depending on their activity and the related near/intermediate/far content [1].

Intersubject differences in preference. We found large intersubject variability in the preferences across lens designs, with each subject revealing a different preference pattern (Fig. 6). While the overall energy in the corrections was the same across the designs, the perceptual blur reported was undeniably different across subjects, due to the different through-focus energy distribution profile of each design, interactions between the native aberrations and the lens design, and, likely, different blur tolerances across individuals. Besides modifying the near add [26] or the balance distribution for near/intermediate/far, it is conceivable to customize the lens design to the patient's preference, or at least consider the patient's preference when selecting the optimal lens.

Neural adaptation. The exposure to a new visual experience (for example, multifocallity) during a certain period of time could potentially change the patients' perceptual judgments. In previous studies, we have investigated neural spatial adaptation. In particular, we have demonstrated that subjects are long-term adapted to their native optical degradation [10,11], and that there are shifts in perception following short periods of adaptation to a new optical experience [16]. We found that neural re-calibration occurs after very short periods of adaptation, which has been considered in the design of the experiments.

Implications. A number of bench prototypes and commercial visual simulators are available based on various optical principles. To our knowledge, this is the only simulator that is based on temporal multiplexing, and that provides a programmable through-focus open-field simulation. Most studies in the literature report [1,5] visual function measurements in eyes already implanted with a given lens design. Visual simulators allow testing multiple designs on the same eye and identifying the optimal selection. Most adaptive optics instruments reported in the literature are either on-bench [13,27–29] or are limited to simulating only one design at a time or visual tests are displayed in a small-field display (not open view) [7,9,30]. The opportunity for simulating commercially available lens designs using a portable see-through device opens the possibility of easily transferring this tool to the clinic to help in identifying the optimal correction.

Limitations and future prospects. The miniaturized simultaneous vision simulator described here simulates a multifocal correction by temporal multiplexing. This rapidly and effectively reproduces any through-focus energy profile, and the measurements are found to be repeatable. These can also reproduce haloes associated with multifocal corrections. However, this technique fails to simulate diffractive effects caused by the concentric rings in the diffractive IOLs or the spatial distribution of the refractive designs. Yet, our results demonstrate that the visual and perceptual outcomes are primarily affected by the far/near energy distribution, hence making the system useful as a screening tool. Further clinical trials will eventually be needed to validate the degree of equivalence between the simulation provided by the instrument and the real multifocal lens implanted.

Some of the limitations can be addressed to some extent by using phase plates or incorporating light modulators used in on-bench prototypes [6,14] to simulate specific effects. In addition, the system can be expanded to a binocular device by replicating a second channel for the contralateral eye. Such a system could simulate not only monocular multifocal corrections but also other presbyopia correction alternatives such as monovision and extended monovision, which involve different corrections in each eye.

5. CONCLUSION

The visual and perceptual performances are affected to a great extent by the far/near energy ratio. Our results show clear intersubject differences in perceptual preference of simultaneous vision correction. The hand-held simultaneous vision simulator based on temporal multiplexing is an effective tool to optically simulate multifocal corrections. Clinical implementation of this technique can make practice of multifocal prescription evidence-based by assessing subjective needs and preferences prior to invasive intervention.

Funding. European Research Council (ERC) (ERC-2011-AdG-294099); Ministerio de Economía y Competitividad (MINECO) (FIS2011-264605, FIS2014-56643-R); Seventh Framework Programme (FP7) (PITN-GA-2010-264605).

REFERENCES

1. R. Bellucci, “Multifocal intraocular lenses,” Curr. Opin. Ophthalmol. **16**, 33–37 (2005).
2. S. Cillino, A. Casuccio, F. Di Pace, R. Morreale, F. Pillitteri, G. Cillino, and G. Lodato, “One-year outcomes with new-generation multifocal intraocular lenses,” Ophthalmology **115**, 1508–1516 (2008).
3. B. Cochener, A. Lafuma, B. Khoshnood, L. Courouve, and G. Berdeaux, “Comparison of outcomes with multifocal intraocular lenses: a meta-analysis,” Clin. Ophthalmol. **5**, 45–56 (2011).
4. M. J. Kim, L. Zheleznyak, S. Macrae, H. Tchah, and G. Yoon, “Objective evaluation of through-focus optical performance of presbyopia-correcting intraocular lenses using an optical bench system,” J. Cataract Refractive Surg. **37**, 1305–1312 (2011).
5. A. Llorente-Guillemot, S. Garcia-Lazaro, T. Ferrer-Blasco, R. J. Perez-Cambrodi, and A. Cervino, “Visual performance with simultaneous vision multifocal contact lenses,” Clin. Exp. Optom. **95**, 54–59 (2012).
6. M. Vinas, C. Dorronsoro, V. Gonzalez, D. Cortes, and S. Marcos, “Testing vision with angular and radial multifocal phase patterns using adaptive optics,” Invest. Ophthalmol. Visual Sci. (to be published).
7. C. Canovas, S. Manzanera, C. Schwarz, P. Prieto, H. A. Weeber, P. A. Piers, and P. Artal, “Binocular performance of IOL combinations studied with a visual simulator,” Invest. Ophthalmol. Visual Sci. **55**, 4024 (2014).
8. E. J. Fernandez, P. M. Prieto, and P. Artal, “Binocular adaptive optics visual simulator,” Opt. Lett. **34**, 2628–2630 (2009).
9. C. Schwarz, P. M. Prieto, E. J. Fernandez, and P. Artal, “Binocular adaptive optics vision analyzer with full control over the complex pupil functions,” Opt. Lett. **36**, 4779–4781 (2011).
10. L. Sawides, P. de Gracia, C. Dorronsoro, M. Webster, and S. Marcos, “Adapting to blur produced by ocular high-order aberrations,” J. Vis. **11**(7), 21 (2011).
11. L. Sawides, P. de Gracia, C. Dorronsoro, M. A. Webster, and S. Marcos, “Vision is adapted to the natural level of blur present in the retinal image,” PLoS One **6**, e27031 (2011).
12. L. Sawides, C. Dorronsoro, P. de Gracia, M. Vinas, M. Webster, and S. Marcos, “Dependence of subjective image focus on the magnitude and pattern of high order aberrations,” J. Vis. **12**(8), 4 (2012).
13. P. de Gracia, C. Dorronsoro, A. Sanchez-Gonzalez, L. Sawides, and S. Marcos, “Experimental simulation of simultaneous vision,” Invest. Ophthalmol. Visual Sci. **54**, 415–422 (2013).
14. C. Dorronsoro, A. Radhakrishnan, P. de Gracia, L. Sawides, and S. Marcos, “Perceived image quality with simulated segmented bifocal corrections,” Biomed. Opt. Express (to be published).
15. A. Radhakrishnan, C. Dorronsoro, and S. Marcos, “Differences in visual quality with orientation of a rotationally asymmetric bifocal IOL design,” J. Cataract Refractive Surg. (to be published).

16. A. Radhakrishnan, C. Dorronsoro, L. Sawides, and S. Marcos, "Short-term neural adaptation to simultaneous bifocal images," PLoS One **9**, e93089 (2014).
17. C. Dorronsoro, J. R. Alonso, and S. Marcos, "Miniature simultaneous vision simulator instrument," Patent WO2015049402 A1 (Apr. 9, 2015).
18. C. Dorronsoro and S. Marcos, "Miniaturized simultaneous vision simulator with mask generator," Spanish patent P201531397 (Oct. 30, 2015).
19. E. Gambra, L. Sawides, C. Dorronsoro, and S. Marcos, "Accommodative lag and fluctuations when optical aberrations are manipulated," J. Vis. **9** (6), 4 (2009).
20. S. Marcos, L. Sawides, E. Gambra, and C. Dorronsoro, "Influence of adaptive-optics ocular aberration correction on visual acuity at different luminances and contrast polarities," J. Vis. **8**(13), 1 (2008).
21. J. Birkenfeld, A. de Castro, and S. Marcos, "Contribution of shape and gradient refractive index to the spherical aberration of isolated human lenses," Invest. Ophthalmol. Visual Sci. **55**, 2599–2607 (2014).
22. J. T. Holladay, "Proper method for calculating average visual acuity," J. Refract. Surg. **13**, 388–391 (1997).
23. W. H. Ehrenstein and A. Ehrenstein, *Psychophysical Methods in Modern Techniques in Neuroscience Research* (Springer, 1999).
24. D. G. Pelli and B. Farell, *Psychophysical Methods in Handbook of Optics* (McGraw-Hill, 1995).
25. R. D. Yates and D. J. Goodman, *Probability and Stochastic Processes: a Friendly Introduction for Electrical and Computer Engineers* (Wiley, 2005).
26. P. de Gracia, C. Dorronsoro, and S. Marcos, "Multiple zone multifocal phase designs," Opt. Lett. **38**, 3526–3529 (2013).
27. C. Dorronsoro and S. Marcos, "Instrument for simulating multifocal ophthalmic corrections," Patent PCT/ES2010/070218 (Apr. 8, 2009).
28. H. Guo, D. A. Atchison, and B. J. Birt, "Changes in through-focus spatial visual performance with adaptive optics correction of monochromatic aberrations," Vis. Res. **48**, 1804–1811 (2008).
29. G. Y. Yoon and D. R. Williams, "Visual performance after correcting the monochromatic and chromatic aberrations of the eye," J. Opt. Soc. Am. A **19**, 266–275 (2002).
30. J. Pujol, M. Aldaba, A. Giner, J. Arasa, and S. Luque, "Visual performance evaluation of new multifocal intraocular design before surgery," Invest. Ophthalmol. Visual Sci. **55**, 3752 (2014).